Systemic Metabolic Alteration Dependent on the Thyroid-Liver Axis in Early PD

Kengo Miyamoto, MS,[1] Shinji Saiki, MD, PhD,[1] Hirotaka Matsumoto, PhD,[2,3] Ayami Suzuki, BS,[1] Yuri Yamashita, MD, PhD,[1,4] Tatou Iseki, MD,[1] Shin-Ichi Ueno, MD, PhD,[1] Kenta Shiina, MD,[1] Tetsushi Kataura, PhD,[1] Koji Kamagata, MD, PhD,[5] Yoko Imamichi, BS,[1] Yukiko Sasazawa, PhD,[6] Motoki Fujimaki, MD, PhD,[1] Wado Akamatsu, MD, PhD,[7] and Nobutaka Hattori, MD, PhD[1]

Objective: Parkinson's disease (PD) is a common neurodegenerative disease characterized by initial involvement of the olfactory bulb/amygdala or autonomic nerves followed by nigral degeneration. Although autonomic innervation strictly regulates multiorgan systems, including endocrine functions, circulation, and digestion, how dysautonomia in PD affects systemic metabolism has not been identified. In this study, we tried to estimate the pathogenic linkage of PD by nuclear medicine techniques, trans-omic analysis of blood samples, and cultured cell experiments.
Methods: Thyroid mediastinum ratio of ^{123}I-metaiodobenzylguanidine (MIBG) scintigraphy was measured in 1,158 patients with PD. Furthermore, serum exosome miRNA transcriptome analysis and plasma metabolome analysis followed by trans-omic analysis were performed in patients with de novo PD and age-matched healthy control persons. Additionally, thyroid hormone was administered to skeletal muscle and liver derived cells to evaluate the effect of hypothyroidism for these organs.
Results: Sympathetic denervation of thyroid correlating with its cardiac denervation was confirmed in 1,158 patients with PD by MIBG scintigraphy. Among patients with drug-naïve PD, comprehensive metabolome analysis revealed decreased levels of thyroxine and insufficient fatty acid β-oxidation, which positively correlate with one another. Likewise, both plasma metabolome data and transcriptome data of circulating exosomal miRNAs, revealed specific enrichment of the peroxisome proliferator-activated receptor (PPARα) axis. Finally, association of thyroid hormone with PPARα-dependent β-oxidation regulation was confirmed by in vitro experiments.
Interpretation: Our findings suggest that interorgan communications between the thyroid and liver are disorganized in the early stage of PD, which would be a sensitive diagnostic biomarker for PD.

ANN NEUROL 2023;93:303–316

Introduction

Parkinson's disease (PD), the second most common neurodegenerative disease, affects approximately 1% of individuals over the age of 60 years and is characterized by typical motor symptoms (bradykinesia, rest tremor, and muscle rigidity) and non-motor symptoms (hyposmia, depression, apathy, sleep disorders, and dysautonomia).[1–4] At least half of the patients with PD have orthostatic hypotension, insufficient gastric emptying, pollakisuria, and/or constipation, even in the early stage of the disease.[5]

View this article online at wileyonlinelibrary.com. DOI: 10.1002/ana.26510

Received Jun 15, 2022, and in revised form Sep 18, 2022. Accepted for publication Sep 19, 2022.

Address correspondence to Dr Saiki, Department of Neurology, Juntendo University School of Medicine, 2-1-1 Hongo, Bunkyo-ku, Tokyo 113-8421, Japan. E-mail: ssaiki@juntendo.ac.jp; Dr Hattori, Department of Neurology, Juntendo University School of Medicine, 2-1-1 Hongo, Bunkyo-ku, Tokyo 113-8421, Japan. E-mail: nhattori@juntendo.ac.jp

From the [1]Department of Neurology, Juntendo University Graduate School of Medicine, Tokyo, Japan; [2]School of Information and Data Sciences, Nagasaki University, Nagasaki, Japan; [3]Laboratory for Bioinformatics Research, RIKEN Center for Biosystems Dynamics Research, Saitama, Japan; [4]Aging Biology in Health and Disease, Juntendo University Graduate School of Medicine, Tokyo, Japan; [5]Department of Radiology, Juntendo University Graduate School of Medicine, Tokyo, Japan; [6]Research Institute for Diseases of Old Age, Juntendo University Graduate School of Medicine, Tokyo, Japan; and [7]Center for Genomic and Regenerative Medicine, Juntendo University Graduate School of Medicine, Tokyo, Japan

Additional supporting information can be found in the online version of this article.

Various functional studies of patients with PD have shown sympathetic and parasympathetic denervation by cardiac ^{123}I-metaiodobenzylguanidine (MIBG) scintigraphy and donepezil positron emission tomography to assess colonic cholinergic innervation, respectively.[6] In addition, phosphorylated alpha-synuclein (αSyn) deposits in autonomic nerve terminals of the skin, salivary glands, and colon mucosa have been identified in patients with prodromal and/or early PD.[7,8] The autonomic nervous system generally governs respiration, circulation, body temperature, and the endocrine systems. Hormones, cytokines, growth factors, and immunoglobulins connect isolated organs throughout the body to regulate whole-body metabolism.[9] Although metabolic changes in amino acids, kynurenine, caffeine, fatty acids (FAs), and polyamines in the serum/plasma of patients with PD have been identified by us and others, those arising from dysautonomia remain unclear.[10-12]

The thyroid is one of the most important organs regulating metabolism of the brain, white fat, brown fat, skeletal muscles, and liver, mainly under control of the hypothalamus-pituitary-thyroid axis.[13] In addition, use of animal models has delineated a functional role for sympathetic innervation on thyroid hormone secretion.[14-17] In humans, blood supplied from the intrathyroidal artery is regulated by sympathetic nerves, mainly from the cervical ganglia along the artery.[13] Sympathetic innervation of the thyroid in healthy humans was confirmed by 6-^{18}F-fluorodopamine imaging with/without desipramine, an inhibitor of serotonin/noradrenaline uptake.[18] In patients with PD, significant decreases of MIBG or 6-^{18}F-fluorodopamine uptake in the thyroid have been identified.[18-20] Horsager et al found that postganglionic autonomic denervation is initiated from celiac or mesenteric ganglions and retrogradely expanded to cervical ganglia in one subtype of PD.[21] Because pharmacologic doses of dopamine, glucocorticoids, and somatostatin suppress thyroid stimulating hormone (TSH),[22] it remains unclear how thyroid function affects downstream target organs, such as skeletal muscle, cardiac muscle, and liver in PD treated with/without L-DOPA and/or dopamine agonists.

Here, we report sympathetic denervation of the thyroid by cardiac MIBG scintigraphy in patients with PD, especially those with constipation, that correlated with cardiac denervation and nigral dopamine degeneration. Moreover, we identified suppression of FA β-oxidation and its positive correlation with thyroxine levels in patients with de novo PD. To investigate interorgan communication, we performed transcriptome analysis of circulating serum exosomal miRNAs, which may serve as mediators among organs and appropriate diagnostic biomarkers for several diseases compared with non-exosomal miRNAs.[23-25] Based on these assays, the peroxisome proliferator-activated receptor (PPARα) axis was enriched. Finally, we confirmed an association between thyroid hormone and the PPARα pathway in the liver using cultured human cell lines, proposing inter-tissue communication in early PD.

Methods

Ethics Statement

This study protocol complied with the Declaration of Helsinki and was approved by the ethics committee of Juntendo University. Written informed consent was given by all participants.

Participants

All participants had been treated at Juntendo University Hospital and were recruited between 2016 and 2020. Written informed consent provided by all participants. PD was diagnosed according to diagnostic criteria of the Movement Disorder Society.[26] Patients with PD and possible dementia (Mini-Mental State Examination score = <24) were excluded to avoid substantial overlap between PD with possible dementia and Alzheimer's disease. Hoehn and Yahr (H&Y) stages and Unified Parkinson's Disease Rating Scale (UPDRS-III) motor section scores were defined during the "on" phase for practical and ethical reasons. To evaluate non-motor symptoms, subjective orthostatic hypotension (OH) and functional constipation according to Rome III criteria[27] were investigated. For MIBG scintigraphy, we recruited patients with PD (n = 1,158) and without PD (non-PD, n = 67) including healthy control (HC) subjects (n = 29), drug-induced parkinsonism (n = 18), and essential tremor (n = 20; Table 1).

For comprehensive metabolome analysis, we recruited 20 patients with de novo PD (unmedicated with any anti-Parkinson drug) and 25 age-matched controls during the same period (2016–2020). In the same cohort, 18 patients with de novo PD and 21 age-matched controls were enrolled for transcriptome analysis (Table 2).

Sample Collection

All fasting blood samples were collected at the outpatient department of Juntendo University Hospital from June 2015 to January 2019. Plasma and serum were extracted as previously described[10] and stored at −80°C until use.

Metabolome Analysis

Using capillary electrophoresis time-of-flight mass spectrometry (MS) and liquid chromatography (LC) time-of-flight MS with Advanced Scan Plus (Human Metabolome Technologies, Yamagata, Japan), comprehensive metabolome

TABLE 1. Demographic characteristics of participants examined MIBG scintigraphy

	Non-PD	PD	*p*	Early PD without constipation	*p*	Early PD with constipation	*p*
Number	67	1,158		114		246	
Sex, M:F	22:45	560:598	**0.0123**[a]	56:58	**0.0314**[a]	113:133	0.0525[a]
Age, yr, mean (SD)	69.4 (11.9)	66.9 (10.4)	**0.0188**[b]	65.6 (10.4)	**0.0159**[b]	69.3 (8.82)	0.617[b]
Disease duration, yr, mean (SD)	-	5.21 (5.54)		1.33 (0.768)		1.33 (0.784)	
H&Y stage, mean (SD)	-	2.06 (0.844)		1.80 (0.770)		1.97 (0.681)	
H&Y stage, (each case number)	-	I (262), II (602), III (174), IV (48), V (18), nd (54)		I (44), II (51), III (15), IV (3), V(0), nd (1)		I (47), II (162), III (25), IV (3), V (3), nd (6)	
Early H/M, mean (SD)	3.06 (0.673)	2.08 (0.673)	**<0.0001**[b]	2.33 (0.703)	**<0.0001**[b]	2.00 (0.641)	**<0.0001**[b]
Delayed H/M, mean (SD)	3.26 (0.873)	1.87 (0.873)	**<0.0001**[b]	2.18 (0.869)	**<0.0001**[b]	1.74 (0.748)	**<0.0001**[b]
Early T/M, mean (SD)	1.49 (0.316)	1.35 (0.219)	**0.0002**[b]	1.42 (0.216)	0.376[b]	1.34 (0.198)	**0.0009**[b]
Delayed T/M, mean (SD)	2.18 (0.856)	1.96 (0.526)	0.0628[b]	2.06 (0.526)	0.936[b]	1.91 (0.473)	**0.0486**[b]
SBR, mean (SD)	5.30 (1.70)	2.45 (1.38)	**<0.0001**[b]	2.87 (1.25)	**<0.0001**[b]	2.60 (1.21)	**<0.0001**[b]
Prevalence of orthostatic hypotension	-	-		9.41% (nd: n = 29)		32.1% (nd: n = 81)	**<0.0001**[c]

Abbreviations: delayed H/M = delayed heart to mediastinum ratio of MIBG scintigraphy; early H/M = early heart to mediastinum ratio of MIBG scintigraphy; early T/M = early thyroid to mediastinum ratio of MIBG scintigraphy; H&Y stage = Hoehn and Yahr staging scale; MIBG = ^{123}I-metaiodobenzylguanidine; nd = not determined; PD = Parkinson's disease; SBR = specific binding ratio of DaT-SPECT; SD = standard deviation.

[a]The *p* values were obtained by chi-squared test compared to non-PD.

[b]The *p* value was obtained by Steel's test compared to non-PD.

[c]The *p* value obtained by chi-squared test comparing each type of early PD.

analysis was conducted based on the methods described previously.[10]

Transcriptome Analysis of miRNAs

Exosomal miRNA was extracted from 1 ml of peripheral blood serum using a Total Exosome RNA and Protein Isolation Kit (Thermo Fisher Scientific, Waltham, MA) according to the manufacturer's protocol. The quality of miRNA in the eluate was checked using Agilent Small RNA Kit and the concentration was measured with an Agilent RNA 6000 Pico Kit with Bioanalyzer (Agilent Technologies).

Small Library Construction and Ion PGM sequencing were conducted at Thermo Fisher Scientific. Small RNA libraries were prepared with an Ion Total RNA-Seq kit version 2 (Thermo Fisher Scientific). Then prepared

TABLE 2. Demographic characteristics of participants in multi-omics analysis

Characteristic	Metabolome			miRNA		
	HCs	De novo PD	*p*	HCs	De novo PD	*p*
Number	25	20		21	18	
Sex, M:F	13:12	8:12	0.422[a]	11:10	8:10	0.621[a]
Age, yr, mean (SD)	63.8 (10.6)	62.8 (10.5)	0.883[b]	64.0 (11.2)	61.7 (10.5)	0.576[b]
Disease duration, yr, mean (SD)	-	1.45 (1.49)		-	1.47 (1.55)	
H&Y stage, mean (SD)	-	1.65 (0.81)		-	1.67 (0.84)	
H&Y stage, (each case number)	-	I (11), II (5), III (4)		-	I (10), II (4), III (4)	
MDS-UPDRS III, mean (range)	-	18.0 (2–44)		-	18.4 (2–44)	
MMSE, mean (SD)	-	28.7 (1.8)		-	28.7 (1.8)	
BMI, kg/m^2, mean (SD)	23.2 (2.9)	22.0 (4.2)	0.212[b]	23.4 (2.9)	22.1 (4.3)	0.208[b]

Abbreviations: BMI = body mass index; H&Y stage = Hoehn and Yahr staging scale; HC = healthy controls; MDS-UPDRS III = the Movement Disorder Society-sponsored revision of the Unified Parkinson's disease rating scale part III; MMSE = Mini Mental State Examination; PD = Parkinson's disease; SD = standard deviation.

[a]*P*-value obtained by Chi-square test.

[b]*P*-value obtained by Steel's test compared to healthy controls.

libraries were sequenced with an Ion 540 kit (Thermo Fisher Scientific) on an Ion PGM System.

Pathway Analysis of Upregulated miRNA

Pathway analysis was performed for 101 upregulated miRNAs in patients with de novo PD using mirPath version 3 followed by TarBase (http://snf-515788.vm.okeanos.grnet.gr/). The threshold for p values was set to less than 0.05.

Trans-Omics Analysis

Following prediction of mRNAs targeted by the significantly changed 141 miRNAs (Table S1) using DIANA-TarBase software, 1,167 mRNAs regulated by 10 or more miRNAs were subjected to subsequent trans-omics analysis. Trans-omics analysis combining those mRNAs with the 63 significantly changed metabolites identified (Table S2) was performed using IMPaLA software (http://impala.molgen.mpg.de/).

^{123}I-Metaiodobenzylguanidine Scintigraphy

Participants were intravenously injected with iodine-123 metaiodobenzylguanidine (^{123}I-MIBG; MyoMIBG-I 123 injection, 111 MBq; FUJIFILM Toyama Chemical Co., Ltd., Tokyo, Japan). Scintigraphic images were acquired by E CAM at 30 minutes (early) and 3 hour (delayed) after injection. Regions of interest for the heart, thyroid, and mediastinum were semi-automatically positioned and quantified using smartMIBG software (FUJIFILM Toyama Chemical Co., Ltd.). H/M and T/M ratios were calculated with the following formulas: H/M ratio = (mean count of the heart uptake)/(mean count of the mediastinum uptake), T/M ratio = (mean count of the thyroid uptake)/(mean count of the mediastinum uptake).

Dopamine Transporter Single-Photon Emission Computed Tomography Imaging

Three hours after injection of approximately 185 MBq of ^{123}I-FP-CIT, projection data were obtained in a 128 × 128 matrix on a Siemens Symbia T16 mounted with low- to medium-energy general purpose collimators (Siemens, Munich, Germany). Projection data were acquired for 28 minutes. Data were reconstructed by the ordered subset expectation maximization method (iteration 8 and subset 6) with Flash 3D software. Specific Binding Ratio (SBR) values were semi-quantitatively calculated using DAT VIEW software (Nihon Medi-Physics, Tokyo, Japan) based on Bolt's method. Here, we calculated SBR as the mean value of right and left SBRs.

Cell Culture and Transfection

Human hepatoma cell line HepG2 cells were cultured in Dulbecco's Modified Eagle's Medium (DMEM; 11,885,084; Thermo Fisher Scientific) supplemented with 10% fetal bovine serum and 100 U/ml penicillin/streptomycin. Human skeletal muscle myoblasts (HSMM) cells

(CC-2580; Lonza, Walkersville, MD) were maintained in SkGM-2 Skeletal Muscle Cell Growth Medium (Lonza) and differentiated to myotubes for 10 to 14 days in DMEM-F12 (12-719F; Lonza) supplemented with 2% horse serum (H1270; Sigma-Aldrich).

For RNA-interference experiments, siRNA oligonucleotides were transfected into HepG2 cells and myotubes using DharmaFECT-4 (Horizon Discovery, Cambridge, UK) and Lipofectamine RNAiMAX (Thermo Fisher Scientific), respectively, according to the manufacturer's instructions. Forty-eight hours after siRNA transfection, the cells were used in the experiments.

Hormonal Stimulation

Cultured cells were washed with phosphate-buffered saline and incubated in 10% thyroid hormone depleted serum (SF231–7; BBI Solutions, Cardiff, UK) and 3,3′,5-triiodo-L-thyronine sodium salt (T6397; Sigma-Aldrich).

RNA Extraction and Real-Time Polymerase Chain Reaction Analysis

Total RNA was isolated using an RNeasy mini Kit (Qiagen, Valencia, CA) and quantified with a NanoDrop 1,000 (Thermo Fisher Scientific). Reverse transcription was carried out with 1 μg of total RNA using a ReverTra Ace qPCR RT kit (FSQ-101; Toyobo, Osaka, Japan) according to the manufacturer's instructions. Real-time polymerase chain reaction (PCR) was performed using Fast SYBR Green Master Mix (Thermo Fisher Scientific) and primers (*GAPDH*: forward [FW]: 5′-TGCACCACCAACTGCTTAGC-3′ and reverse [RV]: 5′-GCATGGACTGTGGTCATGAG-3′, *PPARα*: FW: 5′-CCTGTCTGCTCTGTGGACTC-3′ and RV: 5′-GCTCCAAGCTACTGTGGTGA-3′, *CPT1A*: FW: 5′-CTTTGGACCGGTTGCTGATG-3′ and RV: 5′-GTGCCTTCCAAAGCGATGAG-3′, *CPT1B*: FW: 5′-TACAACAGGTGGTTTGACA-3′ and RV: 5′-CAGAGGTGCCCAATGATG-3′, *PGC1α*: FW: 5′-GGCAGAAGGCAATTGAAGAG-3′ and RV: 5′-TCAAAACGGTCCCTCAGTTC-3′) in a QuantStudio 3 Real-Time PCR System (Thermo Fisher Scientific). The mRNA levels were determined with the standard curve method and normalized to *GAPDH* expression.

Western Blotting

For sodium dodecyl sulfate-polyacrylamide gel electrophoresis (SDS-PAGE), cells were lysed in lysis buffer (25 mM Tris–HCl [pH 7.6], 150 mM NaCl, 1% NP-40, 1% sodium deoxycholate, 0.1% sodium dodecyl sulfate, and protease inhibitor cocktail). Lysates were centrifuged at 15,000 × *g* for 10 minutes at 4°C to remove debris. For immunoblotting, supernatants were subjected to 10 to 20% gradient SDS-PAGE. Proteins were transfected onto a polyvinylidene fluoride membrane and probed with anti-CPT1A (ab128568; Abcam, Cambridge, MA), anti-β-actin (MAB1501; EMD Millipore, Billerica, MA) and anti-GAPDH (ab9485; Abcam) antibodies. This was followed by detection with an LAS-4000 Mini instrument (GE Healthcare, Chicago, IL). Signal intensities were quantified using ImageJ software (https://imagej.nih.gov/ij/index.html).

Free Fatty Acid Measurement

HepG2 cultured medium was centrifuged at 8,000 × *g* for 5 minutes at 4°C. The supernatant was processed with a Free Fatty Acid Assay Kit (ab65341; Abcam), according to the manufacturer's instructions. Cells were lysed in 50 μl of lysis buffer to measure protein concentrations by bicinchoninic acid assay.

Extracellular Flux Analysis

HSMM cells were seeded in XF24 cell culture plates (100867-100; Agilent Technologies) at 4,000 cells per well and differentiated for 14 days, followed by treatment with 100 nM T3. XF Cell Mito stress test compounds (103015-100; Agilent Technologies) were loaded into the assay cartridge. Oxygen consumption measurements were performed using an extracellular flux analyzer (Agilent Technologies). After quantifying oxygen consumption, cells were lysed in 100 μl of lysis buffer to measure protein concentrations.

Statistical Analysis

All statistical analyses were performed using JMP14 (SAS Institute, Tokyo, Japan). The chi-squared test was used to analyze categorical variables. Steel or Wilcoxon tests were used to examine participant characteristics and values of MIBG scintigraphy compared with non-PD. Analysis of variance (ANOVA) was used to assess relationships between H&Y stages and H/M or T/M ratios of MIBG scintigraphy among PD groups. Spearman's rank correlation tests were used to examine relationships between various measurements of patients with PD. One-way analysis of covariance (ANCOVA) was performed to exclude the effects of age or disease duration. For metabolome analysis, when a value was under the limit of detection, we assigned it half the minimum value of its compound. To investigate influence of confounding variables (age, sex, body mass index [BMI], and carnitine level) on each metabolite, multiple regression analysis was performed. The Wilcoxon test was used to evaluate significantly changed metabolites. Student's *t* tests were used to select metabolites and miRNAs for trans-omics analysis.

Results

Participants

Characteristics of study participants are summarized in Table 1. Notably, no thyroidal disease with clinical symptoms was identified in any participant. Characteristics of patients with PD (n = 1,158) and without PD (n = 67: HCs [n = 29], drug-induced parkinsonism [n = 18], and essential tremor [n = 20]) who were examined by MIBG scintigraphy are shown. A mild statistical significance in age at scanning was observed between non-PD and PD groups. On average, PD severity was mild-to-moderate according to the H&Y stage (2.06 ± 0.844) and disease duration (5.21 ± 5.54 years). Early and delayed heart/mediastinum (H/M) ratios were significantly decreased in patients with PD compared with individuals in the non-PD group, consistent with previous reports and well-established criteria.[26,28] Moreover, the SBR of ^{123}I-ioflupane-dopamine transporter (DaT)-single photon emission computed tomography (SPECT) was significantly decreased in patients with PD compared with those in the non-PD group, similar to previous reports.[29] Patients with PD exhibiting onset of motor symptoms within 3 years were defined as "early PD" for further analysis (described later; see Table 1).

Thyroidal MIBG Scintigraphy

Postganglionic sympathetic innervation of the thyroid, whose neurotransmitter is noradrenaline, is dependent on nerve fibers mainly from the superior and middle cervical ganglia, which connect to intermediolateral neurons in the Th1-2 cord.[15] Because dual control of thyroid by TSH and the autonomic nervous system has been suggested (especially in animal studies[30]), we evaluated the thyroid/mediastinum (T/M) ratio to investigate sympathetic denervation of the thyroid in patients with PD. A characteristic MIBG result is shown in Figure 1A, presenting decreased uptake in both the heart and thyroid. In patients with PD, both early H/M ratio and T/M ratio were significantly decreased (Fig 1B), and a significant correlation was identified between these ratios ($p < 0.0001$) (Fig 1C). Moreover, both early H/M and T/M ratios were negatively correlated with disease severity assessed by

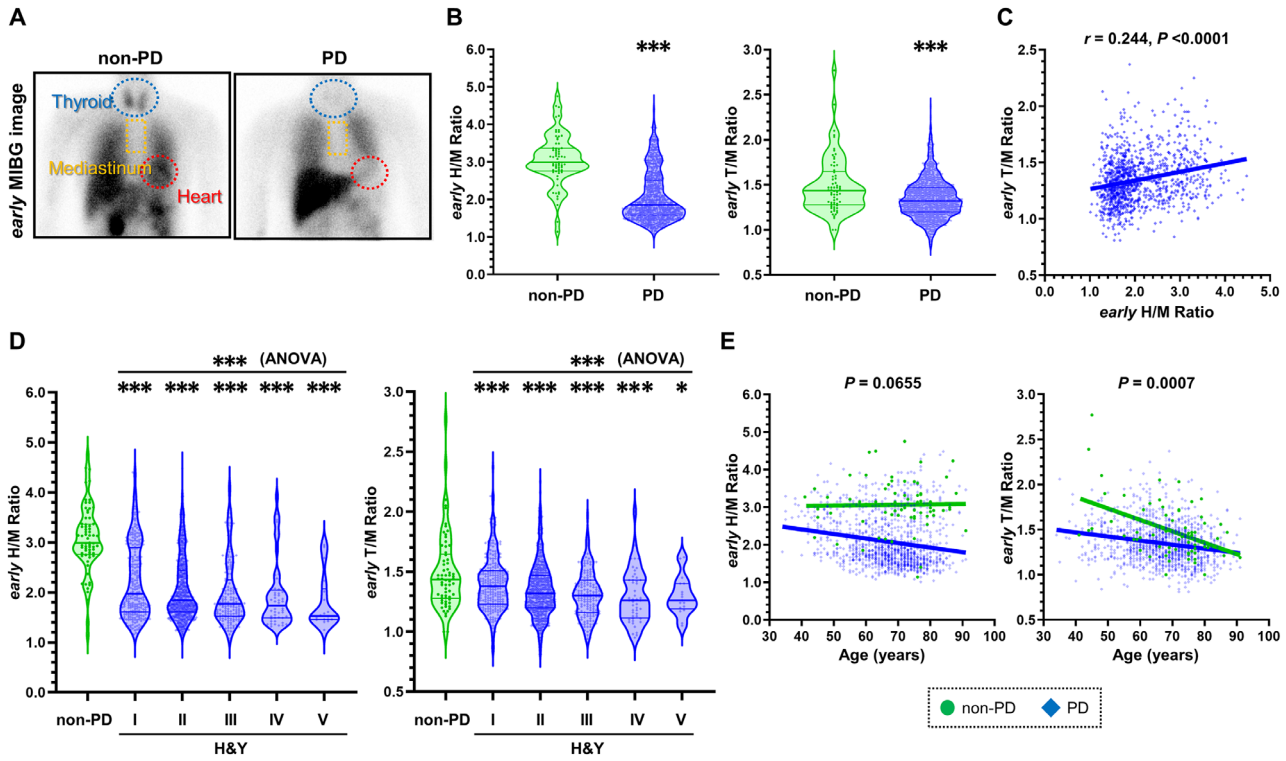

FIGURE 1: Assessments of myocardial and thyroidal MIBG scintigraphy. (A) Early planar images of MIBG scintigraphy in non-PD (*left*) and PD (*right*) groups. Regions of interest were placed on the thyroid (*blue*), heart (*red*), and mediastinum (*yellow*). (B) Comparison between non-PD and PD groups for early heart-to-mediastinum (H/M) or early thyroid-to-mediastinum (T/M) ratios. ***$p < 0.001$ (Wilcoxon's test). (C) Correlation analyses between early H/M ratio and early T/M ratio in patients with PD. The *p* values were obtained by Spearman's rank correlation coefficient. (D) Association of early H/M ratio or early T/M ratio with H&Y stages. *$p < 0.05$, ***$p < 0.001$ (Steel test). (E) Comparison between non-PD and PD groups regarding correlations between age at scanning and early H/M or early T/M ratios. Interaction was assessed by analysis of covariance (ANCOVA) between non-PD and PD groups. ANOVA = analysis of variance; H&Y = Hoehn and Yahr; MIBG = ^{123}I-metaiodobenzylguanidine; PD = Parkinson's disease.

H&Y (Fig 1D). Both early H/M and T/M ratios were decreased in most patients with PD, and the early T/M ratio was typically higher in younger patients (Fig 1E).

Next, to investigate thyroidal denervation specific for the initial stage of PD, we subdivided patients with "early PD" (within 3 years from the onset of motor symptoms) into 2 groups (with/without constipation) to evaluate the association of sympathetic denervation (Fig 2A, see Table 1). Clinically, prevalence of OH in early PD with constipation was significantly higher than in early PD without constipation, indicating systemic autonomic dysfunction in the former subtype (see Table 1). Although significant decreases of early H/M ratios were observed in both groups (Fig 2B), the early T/M ratio was significantly lower only in patients with PD and constipation (Fig 2C). Significant dopaminergic neurodegeneration, as assessed by SBR of DaT, was identified in both phenotypes (Fig 2D). Sympathetic denervation of the thyroid in patients with PD and constipation were significantly correlated with cardiac denervation (Fig 2E) and dopaminergic degeneration (Fig 2F) compared with patients with PD without constipation.

Metabolome Analysis

To clarify metabolic changes derived from dysautonomia, we investigated metabolites correlated with early T/M, a marker of dysautonomia in PD. Secretion of TSH to regulate thyroid hormone release is itself affected by hormones, including somatostatin, leptin, and dopamine.[13,31] Thus, to exclude the effects of circulating dopamine derived from administered levodopa, comprehensive metabolome analysis in 20 patients with de novo PD and 25 age-matched controls was performed (see Table 2). Serum samples taken from 18 patients with de novo PD and 21 HCs were simultaneously subjected to exosome transcriptome analysis of miRNAs. Characteristics of these participants are shown in Table 2. There were no significant differences in sex, age, or BMI between the HCs and

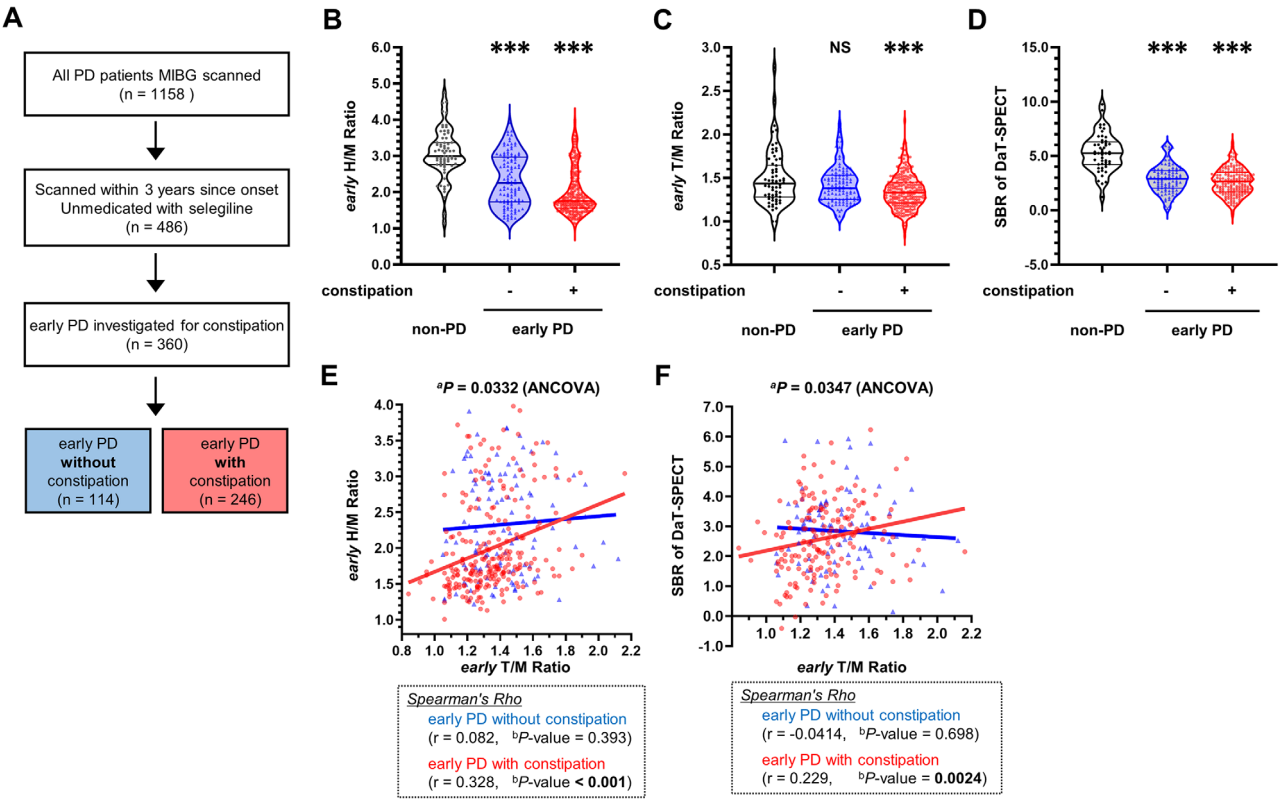

FIGURE 2: Thyroidal MIBG scintigraphy in early PD subgrouped by constipation. (A) Flow of the selection process for the group to investigate thyroidal denervation specific for the initial PD stage. (B-D) Comparison of early H/M ratio (B), early T/M ratio (C) and specific binding ratio (SBR) of DaT-SPECT (D) between non-PD and each type of early PD. ***$p < 0.001$ (Steel test). (E, F) Correlation analyses between early T/M ratio and early H/M ratio (E) and between early T/M ratio and SBR of DaT-SPECT (F) in early PD subgrouped by constipation. Blue triangles represent early PD without constipation and red circles represent early PD with constipation. [a]The p value was calculated by ANCOVA between each type of early PD. [b]The p value was obtained by Spearman's rank correlation coefficient. ANCOVA = analysis of covariance; DaT-SPECT = ^{123}I-ioflupane-dopamine transporter-single photon emission computed tomography; H/M = mean count of the heart uptake/mean count of the mediastinum uptake; MIBG = ^{123}I-metaiodobenzylguanidine; NS = not significant; PD = Parkinson's disease; T/M = mean count of the thyroid uptake/mean count of the mediastinum uptake.

the de novo PD groups. Regarding disease severity, participating patients had shorter disease durations (1.45–1.47 years from onset) and tended to exhibit early-stage PD (mean H&Y stage = 1.65–1.67).

Comprehensive metabolome analysis identified significant changes in 63 metabolites in patients with de novo PD compared with controls, as analyzed by Student's *t* test (see Table S2). Altered metabolites included 17 long-chain FAs (LC-FAs) and 13 long-chain acylcarnitines (LC-ACs). Wilcoxon's test indicated significant decreases in 12 LC-ACs and significant increases in 11 LC-FAs in patients with PD (Table 3). In addition, levels of thyroxine (T4) were significantly decreased in patients with PD ($p = 0.0066$). Notably, Spearman's rank correlation test revealed a significant negative correlation between FAs (the input of β-oxidation) and thyroxine levels, as well as a significant positive correlation between LC-ACs and thyroxine levels, indicating insufficient FA

TABLE 3. Significantly changed metabolites regarding β-oxidation and correlation analysis with thyroxine

			Correlation with thyroxine	
Compound	**Ratio (PD/HC)**	**[a]*p***	***r***	**[b]*p***
AC(12:0)	0.536	**0.0017**	0.153	0.521
AC(12:1)-2	0.664	**0.0020**	0.269	0.252
AC(13:1)	0.565	**0.0116**	0.395	0.0850
AC(14:0)	0.608	**0.0023**	0.519	**0.0190**
AC(14:1)	0.666	**0.0013**	0.289	0.217
AC(14:2)	0.658	**0.0027**	0.328	0.158
AC(15:0)-2	0.764	**0.0055**	0.130	0.586
AC(16:0)	0.684	**0.0001**	0.763	**<0.0001**
AC(16:1)	0.775	**0.0275**	0.382	0.0967
AC(18:0)	0.709	**0.0012**	0.737	**0.0002**
AC(18:1)	0.708	**0.0003**	0.658	**0.0016**
AC(18:2)	0.777	**0.0048**	0.454	**0.0443**
FA(12:0)-2	1.13	**0.0230**	−0.168	0.478
FA(14:1)-3	1.52	**0.0432**	−0.043	0.856
FA(14:3)	1.64	**<0.0001**	0.0137	0.954
FA(17:0)-3	1.18	**0.0259**	−0.192	0.417
FA(17:2)	1.57	**0.0448**	−0.256	0.276
FA(18:2)	1.31	**0.0204**	−0.135	0.571
FA(18:3)	1.37	**0.0456**	−0.283	0.227
FA(19:2)	1.34	**0.0308**	−0.526	**0.0173**
FA(20:2)	1.25	**0.0095**	−0.0206	0.931
FA(20:4)	1.27	**0.0327**	−0.154	0.517
FA(22:4)	1.36	**0.0309**	−0.0160	0.947
thyroxine	0.712	**0.0066**	-	-

Abbreviations: AC = acylcarnitine; FA = fatty acid; HC = healthy controls; PD = Parkinson's disease.
[a]The *p* values were obtained by Wilcoxon's test compared to healthy controls.
[b]The *p* values were obtained by Spearman's rank correlation coefficient analyzed only in PD.

β-oxidation arose from decreased levels of thyroxine in patients with de novo PD (see Table 3). As shown in Figures 3A and 3B, levels of AC(16:0) and ratios of AC(16:0)/FA(16:0) positively correlated with those of thyroxine, consistent with regulation of β-oxidation by thyroxine. Next, to examine the effect of sympathetic denervation on the levels of thyroxine, we performed correlation analysis. Both H/M and T/M ratios tended to correlate with serum thyroxine levels (early H/M ratio: $r = 0.635$, $p = 0.0359$; delayed H/M ratio: $r = 0.543$, $p = 0.0841$; early T/M ratio: $r = 0.828$, $p = 0.0009$; delayed T/M ratio: $r = 0.534$, $p = 0.0697$), with statistical significance detected for early H/M and T/M ratios (Fig 3C). This was consistent with a previous observation of the early T/M ratio being more evident in PD than the delayed T/M ratio.[19] Consistent with this notion, early T/M ratios positively correlated with ratios of AC(16:0)/FA(16:0) (Fig 3D). To adjust effects of confounding variables associated with FA β-oxidation (acylcarnitines, fatty acids, and thyroxine), we performed multiple regression analyses for age, sex, BMI, and serum carnitine levels as confounding variables.[10] Even under these conditions, levels of thyroxine, LC-ACs, and most LC-FAs were significantly altered in PD (Table S3).

Transcriptome Analysis of miRNAs

β-oxidation of LC-FAs is mainly performed in the mitochondria of cardiac muscles, skeletal muscle, and the liver.[10] Extracellular vesicles including exosomes are involved in inter-tissue communication during exercise.[32] Indeed, adipose tissue secretes exosomes containing miRNAs capable of regulating gene expression in the liver and other tissues.[33] Likewise, exosomal miRNAs are candidate messengers among organs that exhibit resistance to degradation in the bloodstream compared with non-exosomal miRNAs.[23,24] Therefore, we hypothesized that miRNAs in exosomes represent an important biologically coordinated mechanism capable of profoundly changing

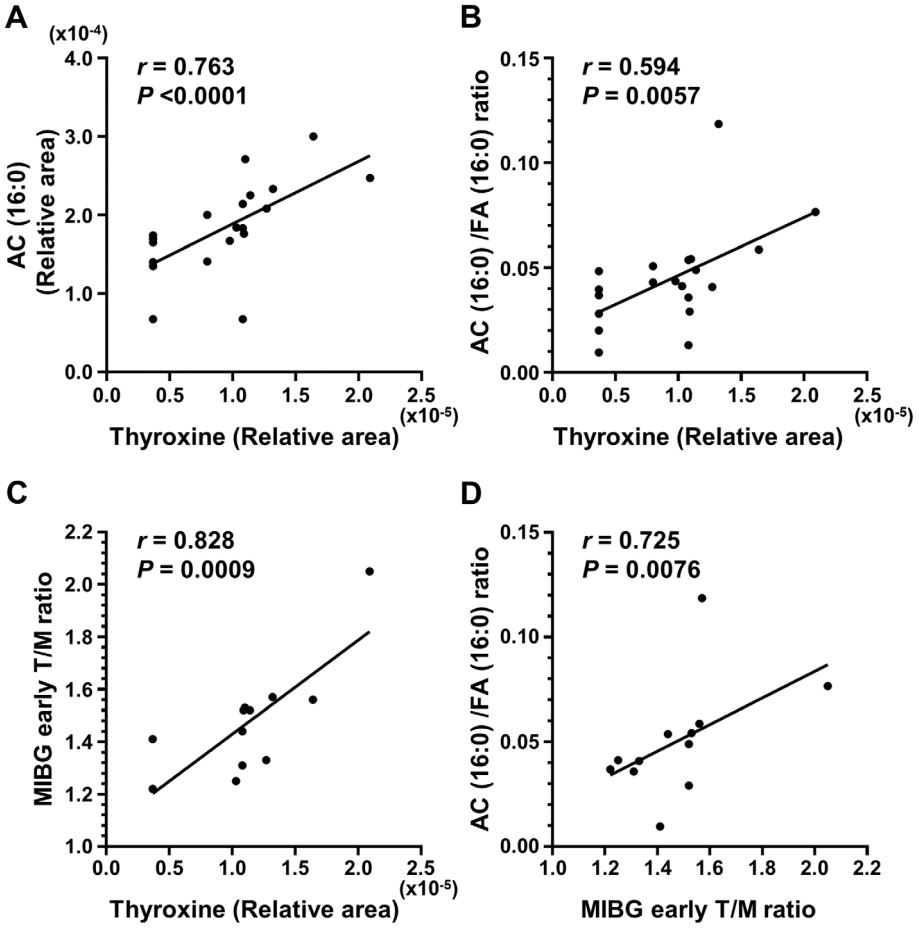

FIGURE 3: Correlation analyses of fatty acid β-oxidation, thyroxine level, and thyroidal MIBG scintigraphy in patients with PD. (A) Correlation between thyroxine level and AC(16:0). (B) Correlation between thyroxine level and AC(16:0)/FA(16:0). (C) Correlation between thyroxine level and early T/M ratio of MIBG scintigraphy. (D) Correlation between early T/M ratio and AC(16:0)/FA(16:0). The *p* value was obtained by Spearman's rank correlation coefficient. AC = acylcarnitine; FA = fatty acid; MIBG = ^{123}I-metaiodobenzylguanidine; T/M = mean count of the thyroid uptake/mean count of the mediastinum uptake.

FA β-oxidation associated with thyroxine decrement. First, comprehensive transcriptome analysis of exosomal miRNAs identified 141 miRNAs significantly altered in patients with PD (see Table S1). Based on miRNA-gene relationships in the DIANA-TarBase version 8 database,[34] we identified 1,167 mRNAs regulated by more than 10 of those miRNAs, which we investigated in subsequent analyses.

In addition, among the 141 miRNAs significantly altered in patients with de novo PD (described above), 101 elevated miRNAs were selected to profile their efficacy. Using DIANA-miRPath version 3.0 followed by TarBase,[35] 67 Kyoto Encyclopedia of Genes and Genomes (KEGG) pathways with p values less than 0.05 including "Fatty acid biosynthesis,", "Thyroid hormone signaling pathway," and "Fatty acid metabolism" were found to be enriched (Table S4). Next, targeted mRNAs within these 3 pathways were identified using mirPath version 3, followed by TarBase (Table S5). Several previous studies investigated circulating exosomal miRNA in plasma or serum of patients with PD,[36-39] and the directions of 6 miRNAs significantly altered in this study were consistent with those reports (hsa-miR-223-5p,[36] miR-652-3p,[37] hsa-miR-181c-5p,[38] hsa-miR-1,273 h-5p,[38] hsa-miR-199b-5p,[38] and miR-338-3p[38]).

Trans-Omics Analysis

To more precisely evaluate systemic changes in patients with PD, trans-omics analysis combining metabolome and transcriptome analyses was performed using IMPaLA.[40] Metabolites and miRNAs identified by trans-omics analysis are listed in Tables S1 and S2. As a result, the PPARα pathway was predicted to be significantly altered in PD, contributing to both metabolomic and transcriptomic changes. Among the pathways identified by IMPaLA,[41] we focused on the PPARα pathway and investigated it using human cell lines because PPARα signaling is closely related to FA metabolism.[41]

In Vitro Study Using Human Cell Models

Altered levels of medium- to LC-ACs and FAs observed in patients with de novo PD might arise from changes of β-oxidation in the liver or skeletal muscles because these metabolic reactions are most active in those organs. To

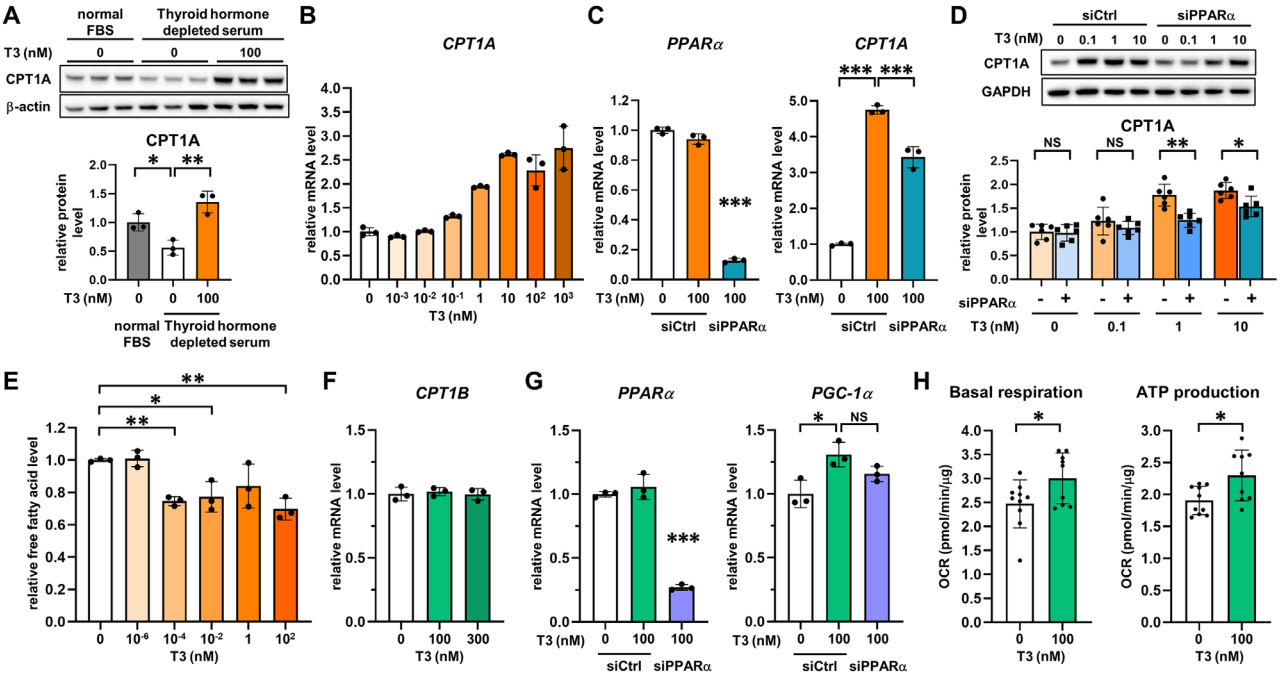

FIGURE 4: The biological effects of T3 on various cell models. (A) CPT1A levels in the hypothyroid condition and with T3 treatment in HepG2 cells. (B) HepG2 cells treated with various concentrations of T3 for 24 hours were analyzed by qRT-PCR. (C) HepG2 cells transfected with PPARα siRNA or control siRNA were treated with 100 nM T3 for 24 hours followed by qRT-PCR. (D) HepG2 cells knockdowned with siPPARα were treated with various concentrations of T3 for 24 hours followed by Western blotting. (E) The levels of free fatty acid in the culture supernatant of HepG2 cells treated with various concentrations of T3 for 24 hours were quantified using Free Fatty Acid Assay Kit (ab65341). (F) Differentiated HSMM cells were treated with indicated concentrations of T3 for 24 hours followed by qRT-PCR. (G) Differentiated HSMM cells transfected with PPARα siRNA or control siRNA were treated with 100 nM T3 for 24 hours followed by qRT-PCR. (H) Differentiated HSMM cells were treated with 100 nM T3 for 72 hours followed by extracellular flux analysis. Data are shown as mean ± SD (n = 3 [A, B, C, E, F, and G], n = 6 [D] n = 9 [H]), *$p < 0.05$, **$p < 0.01$, ***$p < 0.001$ (A, C, and G: Tukey's honest significant difference test, D: Wilcoxon's test, E and H: Dunnett's test). FBS = fetal bovine serum; HSMM = human skeletal muscle myoblast; NS = not significant; qRT-PCR = quantitative real-time polymerase chain reaction.

investigate which organs are important for these changes and the involvement of thyroid hormones and PPARα signaling, we used human hepatocellular carcinoma line HepG2 cells and primary human skeletal myotubular cells. Triiodothyronine (T3) was used for subsequent cell-based assays because local activation of thyroxine (T4) to its active form T3 by 5′-deiodinase 2 is a key mechanism by which thyroid hormone regulates metabolism.[13] Although the thyroid gland produces and releases both T3 and T4, T3 generally possesses several times the biological activity of T4.

In HepG2 cells, T3 increased expression of the carnitine palmitoyltransferase 1A (*CPT1A*) gene, the liver isoform, were significantly decreased in medium containing thyroid hormones depleted serum (Fig 4A) and were increased by the addition of T3 in an almost dose-dependent manner (Fig 4B). The CPT1 enzyme catalyzes the rate-limiting step of FA conversion to acyl-CoA, which is necessary for it to penetrate the mitochondrial outer membrane for subsequent reaction. Levels of *CPT1A* mRNA were partially but significantly suppressed in T3-treated cells following siRNA knockdown of PPARα (Fig 4C). Moreover, CPT1A protein levels were suppressed by PPARα knockdown (Fig 4D). In addition, T3 decreased the level of free FAs in the culture medium of HepG2 cells, which might be a consequence of increased intracellular β-oxidation and FA consumption (Fig 4E).

In human skeletal myotubular cells, T3 did not elevate expression levels of the *CPT1B* gene, the skeletal muscle isoform of CPT1 (Fig 4F). However, T3 could increase the expression level of peroxisome proliferator-activated receptor γ coactivator-1α (*PGC1α*) gene (Fig 4G), which is regulated by thyroid hormones.[42] Consistent with the function of PGC1α in regulating expression of a broad range of genes involved in energy metabolism (including oxidative phosphorylation[43]), T3 significantly enhanced mitochondrial basal respiration and ATP production measured by an extracellular flux analyzer (Fig 4H). Considering that T3 effects on PGC1α expression were not cancelled by PPARα knockdown (see Fig 4G), PGC1α was upregulated by T3 independent of the PPARα pathway in human skeletal myotubular cells. Taken together, the results suggest that thyroid hormone regulates PPARα-mediated CPT1 expression, leading to FA β-oxidation mainly in the liver.

Discussion

In summary, we identified significant thyroidal sympathetic denervation that correlated with cardiac denervation detected by cardiac MIBG scintigraphy in patients with PD. Identification of thyroidal denervation was correlated with cardiac denervation and dopaminergic degeneration in patients with early PD and constipation, but not in patients with PD without constipation. Trans-omics analysis of plasma metabolome and serum exosomal miRNA transcriptome in patients with de novo PD (without medication) showed enrichment of the PPARα pathway based on suppressed FA β-oxidation, as well as hypothyroidism. Finally, we confirmed the presence of a thyroid-PPARα-liver axis using in vitro experiments.

Based on a theory suggested by Horsager et al,[21] our results can be explained by a systemic pattern of neurodegeneration in patients with early PD and constipation (Fig 5). In this phenotype, gut pathologies (such as αSyn accumulation or inflammation) initially result in sympathetic denervation of the superior coeliac ganglion/superior mesenteric ganglion (1). After reaching the sympathetic trunk/intermediolateral nucleus (2), denervation expands retrogradely to the stellate ganglion (3). Subsequently, sympathetic nerves innervating the heart (4) and thyroid (5) are affected. The pathogenic sequence of the gut to the sympathetic ganglion to the heart is widely conceptualized, but the sympathetic noradrenergic lesion in the heart preceding that in the ganglia does not sit well with the pathogenic sequence.[44,45] Likewise, the possibility remains that the pathological role of α-Syn deposition in the sympathetic nerves may be specific to the heart.[46] Further research is required to resolve these issues.

In addition to strict regulation by the hypothalamus-pituitary-thyroid axis,[47] noradrenaline (whose stable analogue is MIBG) exerts a direct stimulatory influence of

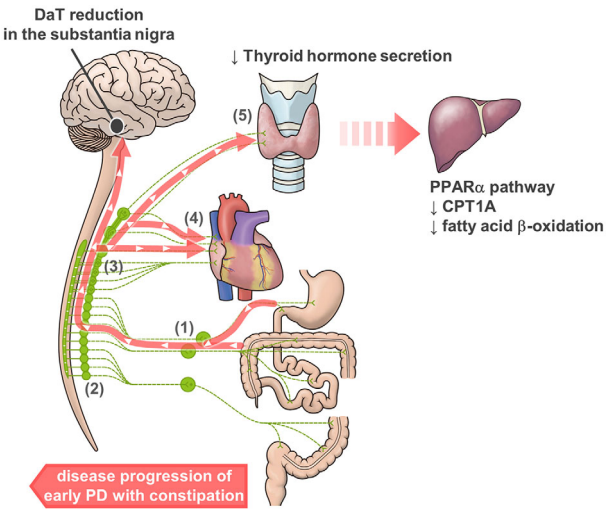

FIGURE 5: Schematic diagram of pathological progression in the sympathetic nervous system in early PD with constipation. (1) = celiac ganglion/superior mesenteric ganglion, (2) = sympathetic trunk, (3) = stellate ganglion, (4) = heart, and (5) = thyroid. DaT = ^{123}I-ioflupane-dopamine transporter; PD = Parkinson's disease.

the sympathetic nervous system on thyroid hormone secretion.[48,49] Because no significant differences in T/M ratio of MIBG imaging were observed between humans treated with or without thyroidal blockade by potassium perchlorate or Lugol's solution, MIBG uptake in the thyroid primarily reflects sympathetic neuronal activity.[50] The present study showed decreased MIBG uptake by the thyroid and its correlation with H/M ratios in patients with early PD, consistent with previous reports.[19,20,28,50] Sympathetic innervation to the heart controls systolic blood pressure in response to posture change and is much denser than that of the thyroid, as evaluated by 6-^{18}F-fluorodopamine imaging.[51,52] In the same report, 100% of patients with PD with OH had abnormal blood pressure responses to the Valsalva maneuver as well as less ventricular 6-^{18}F-fluorodopamine uptake, whereas 26.1% and 47.8% of patients with PD without OH had abnormal Valsalva responses and diffusely decreased 6-^{18}F-fluorodopamine uptake, respectively.[51] Likewise, the serum levels of thyroid hormones were modestly decreased in de novo PD.[28] However, the basis for greater loss of radioactivity in the heart than the thyroid is unknown.

Compared with patients with early PD without constipation, early T/M ratios in patients with early PD and constipation were significantly and positively correlated with H/M ratios, implying progressive involvement of the sympathetic nervous system in a caudo-rostral pattern.[6,21] Consistent with this, prevalence of OH was significantly higher in early PD with OH than in early PD without OH. However, recent analysis of 2 independent cohorts indicates a cholinergic origin of constipation in de novo PD. Thus, the involvement of the parasympathetic nervous system, including the vagal nerve, should be considered for further analysis using ^{11}C-donepezil positron emission tomography-computed tomography.[53]

In our previous study, FA β-oxidation insufficiency indicated by decreased levels of LC-ACs and increased levels of LC-FAs was detected in patients with early-stage PD (H&Y I-II) prescribed medication and patients with de novo PD.[10] These findings are completely reconfirmed by results of the present metabolome analysis. In addition, levels of LC-ACs were correlated with those of thyroxine, whereas LC-FAs were inversely correlated with those of thyroxine, suggesting that FA β-oxidation is under supervision of the thyroid. This finding is further supported by enrichment of the PPARα axis in trans-omics analysis. Extracellular miRNAs in extracellular vesicles, such as exosomes, of body fluids are recognized mediators of intercellular communication even beyond organ boundaries.[23] PPARα signaling is involved in modulation of hepatic lipid metabolism by thyroid hormones and regulated by exosomal 4 miRNAs between adipose tissues and the liver in mice.[25,41] Experimentally, we found that the T3-β-oxidation axis was regulated by CPT1A expression and identified a T3-FA axis in hepatic cell lines. Although T3 upregulated mitochondrial respiration regulated by PGC1α expression, it did not upregulate β-oxidation in a primary skeletal muscle cell line. Accordingly, we propose that insufficient FA β-oxidation arises from thyroid-liver interorgan discoordination in patients with de novo PD; however, there remains a possibility that the effects of thyroid hormone on adipose tissue function and lipid metabolism are deregulated through a hypothalamus-pituitary-thyroid-adipose tissue axis.[54]

Thyroid hormones and PPARα signaling act directly and indirectly on nerves to elicit neuroprotective effects.[55,56] Treatment with thyroid hormone restored dopaminergic neurons differentiated from rat or human neural precursor cells from neurotoxin-induced damage.[55] Moreover, pemafibrate, a selective PPARα modulator, indirectly protected mice against retinal neurodegeneration by modulating balance of serum lipid metabolism via promoting liver functions.[56] Therefore, decreasing thyroid hormone levels and reducing PPARα signaling may induce systemic insults toward both the body and brain.

Exosomal miRNAs reportedly more reliably reflect the state of parental cells than non-exosomal miRNAs as diagnostic biomarkers for pathophysiological studies.[23] Moreover, several studies have reported increased pathological miRNAs in exosomes that, once released from pathogenic cells, can affect distant organs.[57,58] In this study, pathway enrichment analysis of upregulated miRNAs indicated alterations in FA biosynthesis and thyroid signaling, consistent with other clinical signatures, such as insufficient FA β-oxidation due to declined thyroid function.

Some limitations of this study should be considered. First, PD diagnoses were acquired in a single university hospital. Second, the time scale of MIBG measurements was optimized for cardiac sympathetic imaging and, thus, may be inadequate for the thyroid gland. Third, liquid chromatography-mass spectrometry/capillary electrophoresis-mass spectrometry could measure only plasma levels of thyroxine. Fourth, because of the limited number of recruited patients with de novo PD, even in the same recruitment period, there were discrepancies in sample size, therefore, we cannot completely exclude reporting bias.

Acknowledgments

This work was supported by Grants-in-Aid for Scientific Research (S.S., 15H04843, 18H02744, 18KT0027, 18KK0242, 22H02986, and 22K19512), grants from the Japan Agency for Medical Research and Development

(program for Brain Mapping by Integrated Neurotechnologies for Disease Studies [Brain/MINDS], GAPFREE [19ak0101112h0001]), a grant from Japan Science and Technology Agency (Moonshot R&D - MILLENNIA Program, JPMJMS2024), and Supported Program for the Strategic Research Foundation at Private Universities. We thank the Laboratory of Molecular and Biochemical Research, Research Support Center, Juntendo University Graduate School of Medicine, and the support staff of Thermo Fisher Scientific for technical assistance. We thank Edanz (https://jp.edanz.com/ac) for editing a draft of this manuscript.

Author Contributions

K.M. and S.S. contributed to the conception and design of the study. K.M., S.S., H.M., A.S., Y.Y., T.I., S.I.U., K.S., T.K., K.K., Y.I., Y.S., M.F., W.A., and N.H. contributed to the acquisition and analysis of data. K.M. and S.S. contributed to drafting the text and preparing the figures.

Potential Conflicts of Interest

The authors declare no competing interests.

References

1. Bloem BR, Okun MS, Klein C. Parkinson's disease. Lancet 2021;397:2284–2303.
2. Sauerbier A, Jenner P, Todorova A, Chaudhuri KR. Non motor subtypes and Parkinson's disease. Parkinsonism Relat Disord 2016;22:S41–S46.
3. Marras C, Chaudhuri KR. Nonmotor features of Parkinson's disease subtypes. Mov Disord 2016;31:1095–1102.
4. Titova N, Padmakumar C, Lewis SJG, Chaudhuri KR. Parkinson's: a syndrome rather than a disease? J Neural Transm 2017;124:907–914.
5. Schapira AHV, Chaudhuri KR, Jenner P. Non-motor features of Parkinson disease. Nat Rev Neurosci 2017;18:435–450.
6. Horsager J, Andersen KB, Knudsen K, et al. Brain-first versus body-first Parkinson's disease: a multimodal imaging case-control study. Brain 2020;143:3077–3088.
7. Andreasson M, Svenningsson P. Update on alpha-synuclein-based biomarker approaches in the skin, submandibular gland, gastrointestinal tract, and biofluids. Curr Opin Neurol 2021;34:572–577.
8. Sharabi Y, Vatine GD, Ashkenazi A. Parkinson's disease outside the brain: targeting the autonomic nervous system. Lancet Neurol 2021;20:868–876.
9. Lopez-Otin C, Kroemer G. Hallmarks of health. Cell 2021;184:33–63.
10. Saiki S, Hatano T, Fujimaki M, et al. Decreased long-chain acylcarnitines from insufficient beta-oxidation as potential early diagnostic markers for Parkinson's disease. Sci Rep 2017;7:7328.
11. Havelund JF, Heegaard NHH, Faergeman NJK, Gramsbergen JB. Biomarker research in Parkinson's disease using metabolite profiling. Metabolites 2017;7:42.
12. Saiki S, Sasazawa Y, Fujimaki M, et al. A metabolic profile of polyamines in parkinson disease: a promising biomarker. Ann Neurol 2019;86:251–263.
13. Mullur R, Liu YY, Brent GA. Thyroid hormone regulation of metabolism. Physiol Rev 2014;94:355–382.
14. Engeland WC. *Handbook of Clinical Neurology Autonomic Nervous System*. Amsterdam: The Netherlands, Elsevier, 2013:37-44.
15. Grunditz T, Hakanson R, Sundler F, Uddman R. Neuronal pathways to the rat thyroid revealed by retrograde tracing and immunocytochemistry. Neuroscience 1988;24:321–335.
16. Melander A, Ericson LE, Sundler F, Ingbar SH. Sympathetic innervation of the mouse thyroid and its significance in thyroid hormone secretion. Endocrinology 1974;94:959–966.
17. Young JB, Burgi-Saville ME, Burgi U, Landsberg L. Sympathetic nervous system activity in rat thyroid: potential role in goitrogenesis. Am J Physiol Endocrinol Metab 2005;288:E861–E867.
18. Tipre DN, Goldstein DS. Cardiac and extracardiac sympathetic denervation in Parkinson's disease with orthostatic hypotension and in pure autonomic failure. J Nucl Med 2005;46:1775–1781.
19. Matsui H, Udaka F, Oda M, et al. Metaiodobenzylguanidine (MIBG) uptake in Parkinson's disease also decreases at thyroid. Ann Nucl Med 2005;19:225–229.
20. Jang W, Kim JS, Cho JW, et al. Thyroid MIBG uptake in Parkinson's disease with diabetes mellitus. Clin Auton Res 2013;23:221–224.
21. Horsager J, Knudsen K, Sommerauer M. Clinical and imaging evidence of brain-first and body-first Parkinson's disease. Neurobiol Dis 2022;164:105626.
22. Jameson JL, Mandel SJ, Weetman AP. Thyroid gland physiology and testing. In: Jameson JL, Fauci AS, Kasper DL, et al., eds. *Harrison's Principles of Internal Medicine, 20e*. New York, NY: McGraw-Hill Education, 2018;6478:446-449.
23. Kalluri R, LeBleu VS. The biology, function, and biomedical applications of exosomes. Science 2020;367.
24. Nik Mohamed Kamal N, Shahidan WNS. Non-Exosomal and Exosomal circulatory MicroRNAs: which are more valid as biomarkers? Front Pharmacol 2019;10:1500.
25. Castano C, Kalko S, Novials A, Parrizas M. Obesity-associated exosomal miRNAs modulate glucose and lipid metabolism in mice. Proc Natl Acad Sci U S A 2018;115:12158–12163.
26. Postuma RB, Berg D, Stern M, et al. MDS clinical diagnostic criteria for Parkinson's disease. Mov Disord 2015;30:1591–1601.
27. Longstreth GF, Thompson WG, Chey WD, et al. Functional bowel disorders. Gastroenterology 2006;130:1480–1491.
28. Umehara T, Matsuno H, Toyoda C, Oka H. Thyroid hormone level is associated with motor symptoms in de novo Parkinson's disease. J Neurol 2015;262:1762–1768.
29. Bajaj N, Hauser RA, Grachev ID. Clinical utility of dopamine transporter single photon emission CT (DaT-SPECT) with (123I) ioflupane in diagnosis of parkinsonian syndromes. J Neurol Neurosurg Psychiatry 2013;84:1288–1295.
30. Ahren B. Thyroid neuroendocrinology: neural regulation of thyroid hormone secretion. Endocr Rev 1986;7:149–155.
31. Scanlon MF, Weightman DR, Shale DJ, et al. Dopamine is a physiological regulator of thyrotrophin (TSH) secretion in normal man. Clin Endocrinol 1979;10:7–15.
32. Whitham M, Parker BL, Friedrichsen M, et al. Extracellular vesicles provide a means for tissue crosstalk during exercise. Cell Metab 2018;27:237–51.e4.
33. Thomou T, Mori MA, Dreyfuss JM, et al. Adipose-derived circulating miRNAs regulate gene expression in other tissues. Nature 2017;542:450–455.

34. Karagkouni D, Paraskevopoulou MD, Chatzopoulos S, et al. DIANA-TarBase v8: a decade-long collection of experimentally supported miRNA-gene interactions. Nucleic Acids Res 2018;46:D239–D245.

35. Vlachos IS, Zagganas K, Paraskevopoulou MD, et al. DIANA-miRPath v3.0: deciphering microRNA function with experimental support. Nucleic Acids Res 2015 Jul 1;43:W460–W466.

36. Manna I, Quattrone A, De Benedittis S, et al. Exosomal miRNA as peripheral biomarkers in Parkinson's disease and progressive supranuclear palsy: a pilot study. Parkinsonism Relat Disord 2021;93: 77–84.

37. Nie C, Sun Y, Zhen H, et al. Differential expression of plasma Exo-miRNA in neurodegenerative diseases by next-generation sequencing. Front Neurosci 2020;14:438.

38. Cai M, Chai S, Xiong T, et al. Aberrant expression of circulating MicroRNA leads to the dysregulation of alpha-synuclein and other pathogenic genes in Parkinson's disease. Front Cell Dev Biol 2021;9: 695007.

39. He S, Huang L, Shao C, et al. Several miRNAs derived from serum extracellular vesicles are potential biomarkers for early diagnosis and progression of Parkinson's disease. Transl Neurodegener 2021; 10:25.

40. Kamburov A, Cavill R, Ebbels TM, et al. Integrated pathway-level analysis of transcriptomics and metabolomics data with IMPaLA. Bioinformatics 2011;27:2917–2918.

41. Sinha RA, Singh BK, Yen PM. Direct effects of thyroid hormones on hepatic lipid metabolism. Nat Rev Endocrinol 2018;14:259–269.

42. Wulf A, Harneit A, Kroger M, et al. T3-mediated expression of PGC-1alpha via a far upstream located thyroid hormone response element. Mol Cell Endocrinol 2008;287:90–95.

43. LeBleu VS, O'Connell JT, Gonzalez Herrera KN, et al. PGC-1alpha mediates mitochondrial biogenesis and oxidative phosphorylation in cancer cells to promote metastasis. Nat Cell Biol 2014;16:992–1003.

44. Orimo S, Uchihara T, Nakamura A, et al. Axonal alpha-synuclein aggregates herald centripetal degeneration of cardiac sympathetic nerve in Parkinson's disease. Brain 2008;131:642–650.

45. Orimo S, Takahashi A, Uchihara T, et al. Degeneration of cardiac sympathetic nerve begins in the early disease process of Parkinson's disease. Brain Pathol 2007;17:24–30.

46. Isonaka R, Sullivan P, Goldstein DS. Pathophysiological significance of increased alpha-synuclein deposition in sympathetic nerves in Parkinson's disease: a post-mortem observational study. Transl Neurodegener 2022;11:15.

47. Werner SC, Ingbar S. *The Thyroid: A Fundamental and Clinical Text 11th*. Philadelphia: Lippincott Williams & Wilkins, 2020:9-10.

48. Melander A, Ljunggren JG, Norberg KA, et al. Sympathetic innervation and noradrenaline content of normal human thyroid tissue from fetal, young, and elderly subjects. J Endocrinol Invest 1978;1: 175–177.

49. Sundler F, Grunditz T, Hakanson R, Uddman R. Innervation of the thyroid. A study of the rat using retrograde tracing and immunocytochemistry. Acta Histochem Suppl 1989;37:191–198.

50. Giubbini R, Milan E, Marcassa C, et al. 1-23I-MIBG thyroid uptake: implications for MIBG imaging of the heart. J Nucl Cardiol 2016;23: 1335–1339.

51. Goldstein DS, Holmes CS, Dendi R, et al. Orthostatic hypotension from sympathetic denervation in Parkinson's disease. Neurology 2002;58:1247–1255.

52. Espay AJ, LeWitt PA, Kaufmann H. Norepinephrine deficiency in Parkinson's disease: the case for noradrenergic enhancement. Mov Disord 2014;29:1710–1719.

53. Leta V, Urso D, Batzu L, et al. Constipation is associated with development of cognitive impairment in de novo Parkinson's disease: a longitudinal analysis of two international cohorts. J Parkinson's Dis 2021;11:1209–1219.

54. Werner SC, Ingbar S. *The Thyroid: A Fundamental and Clinical Text 11th*. Philadelphia, Lippincott Williams & Wilkins, 2020:446-449.

55. Lee EH, Kim SM, Kim CH, et al. Dopamine neuron induction and the neuroprotective effects of thyroid hormone derivatives. Sci Rep 2019;9:13659.

56. Tomita Y, Lee D, Miwa Y, et al. Pemafibrate protects against retinal dysfunction in a murine model of diabetic retinopathy. Int J Mol Sci 2020;6451:21.

57. Chen L, Han Y, Li Y, et al. Hepatocyte-derived exosomal MiR-194 activates PMVECs and promotes angiogenesis in hepatopulmonary syndrome. Cell Death Dis 2019;10:853.

58. Zhuang G, Wu X, Jiang Z, et al. Tumour-secreted miR-9 promotes endothelial cell migration and angiogenesis by activating the JAK-STAT pathway. EMBO J 2012;31:3513–3523.